

## NUMERICAL ASSESSMENT OF BLAST EFFECTS SCALING PROCEDURES

**Bibiana M. Luccioni<sup>a,c</sup> and Daniel Ambrosini<sup>b,c</sup>**

<sup>a</sup>*Instituto de Estructuras, Universidad Nacional de Tucumán, Av. Roca 1800, 4000 S.M. de Tucumán ,  
Argentina, [bluccioni@herrera.unt.edu.ar](mailto:bluccioni@herrera.unt.edu.ar), [www.herrera.unt.edu.ar/iest](http://www.herrera.unt.edu.ar/iest)*

<sup>b</sup>*Facultad de Ingeniería, Universidad Nacional de Cuyo, Centro Universitario - Parque Gral. San  
Martín - 5500 Mendoza, [dambrosini@uncu.edu.ar](mailto:dambrosini@uncu.edu.ar) , <http://fing.uncu.edu.ar/>*

<sup>c</sup>*CONICET, Av Rivadavia 1917, Cdad de Bs As*

**Keywords:** Explosion, Blast Wave, Crater, Scaling, Numerical simulation.

**Abstract.** Scaling laws are nowadays frequently used for the evaluation of the effects of explosions on structures and soils. They are mainly used to extrapolate results obtained in reduced scale tests to the actual scale case and they are also assumed valid when empirical equations or graphics involving the scaled distance or other scale parameters are used to compute blast effects.

Nevertheless, it has been observed in different works that it is difficult to scale the complete problem including the material micro and meso structure. Moreover, it has been suggested that scaling laws are not the same for all masses, shapes and locations of explosive.

The use of scaling laws for blast effects is numerically assessed in this paper with a hydrocode. Two main applications of blast scaling are analyzed: a) blast wave and its effect on structures and b) crater formation. The accuracy of numerical simulations and numerical results mesh dependence are also addressed in the paper.

First a brief description of most widely used scaling laws for blast effects is presented. The numerical tool and models used are described and the results of the simulation of different scaling cases study are presented. Numerical results are analyzed and compared with experimental results available in blast research literature. The paper is completed with conclusions about the applicability of scaling laws and the accuracy of numerical simulation of the reduced and full scale blast problems for the two types of problems analyzed.

## 1 INTRODUCTION

Extensive research activities in the field of blast loads have taken place in the last few decades. Explosive blast research is important not only for the understanding of damage caused by explosions but also for predicting vulnerability of structures and human to blast and for the development of blast-resistant materials and protective elements (Hargather and Settles, 2009)

Full-scale experiments involving actual geometries and charges are quite involved and costly, both in terms of preparation and measurements. Moreover, full scale testing of realistic urban blast scenarios is often prohibitively expensive and time consuming. Even the smallest of these full-scale tests can require explosive charges of more than 100kg at distances usually greater than 100 m, that is, explosives in the medium to extreme categories and outdoor laboratory experimentation (Nurick et al., 2006). At this scale, instrumentation becomes difficult and expensive, often yielding only point-wise piezoelectric pressure profiles at limited locations and a qualitative rather than quantitative evaluation of material deformation (Hargather and Settles, 2009)

For these reasons, scaled-down experiments are highly desirable. However, the validity of such experiments has to be probed and this is the main objective of this paper.

Most laboratory-scale research focuses on the deformation of plates subjected to blast loads. Nurick et al. (1996) performed most of the initial work and established standard terms for the qualitative classification of plate failure modes and plate deformation measurement (Nurick and Martin, 1989).

Neuberger et al (2007a) presents experimental and numerical results showing that structural response of plates can be modeled and scaled down using geometrical scale together with Hopkinson's (cube root) scaling. Scaling the actual problem appears to be unaffected by the rate-sensitivity of steel. A scaling procedure for the dynamic deformation of constrained steel circular plates subjected to large explosions of flush buried spherical charges has been assessed with respect to experimental results in a second paper (Neuberger et al., 2007b). It was concluded that the problem can be successfully scaled down.

Recently Hargather and Settles (2009) probed the ability to scale material deformations of different materials under explosion loads. In other paper (Hargather et al, 2009b ) they show how blast parameters such as overpressure, duration, and impulse affect the deformation response of a clamped aluminum plate, and how the process might be scaled.

However, there are some recent works showing that scaling is not straightforward in all blast events. Based on experimental results of large and spread explosions, Chung Kim Yuen et al. (2008) showed that, while cube root scaled distance works well for a relatively compact charge layout, the scaled distance parameter should be modified to a fourth root for cases when charges are spread in a carpet-like fashion. Accordingly, based on a numerical analysis of large an spread explosions, Luccioni et al. (2010) recently confirmed that statement and demonstrated that existing empirical formula for the prediction of crater diameter based on cubic root of the explosive mass are not adequate for explosive masses greater than 3500 kg. New expressions covering all the range of explosives masses, from small to extreme cases, were proposed.

The use of scaling laws for blast effects is numerically assessed in this paper with a hydrocode. Two main applications of blast scaling are analyzed: a) blast wave propagation when some reflections are present and b) crater formation. The accuracy of numerical simulations and numerical results mesh dependence are also addressed in the paper.

## 2 BASIC BLAST SCALING THEORY

The principles of scaling and the basic relationships between the small scale model (s) parameters and the full-scale problem (f) parameters (Jones, 1989, Neuberger et al., 2007a) are listed in Table 1.

Scaling Factor	$s$
Linear dimensions	$x_i^s = x_i / s$
Densities	$\rho_i^s = \rho_i$
Stress	$\sigma_{ij}^s = \sigma_{ij}$
Strain	$\varepsilon_{ij}^s = \varepsilon_{ij}$
Characteristic time	$\tau^s = \tau / s$
Loads acting at scaled distances	$F_i^s = F_i$
Displacements of scaled positions and scaled time $t^s = t / s$	$\delta_i^s = \delta / s$

Table 1: Basic scaling relationships

Gravitational forces cannot be scaled according to these basic principles but gravitational forces can be neglected in most blast problems. Material properties are taken to be approximately scale-independent (Neuberger et al 2007a).

The most widely used approach for blast wave scaling is Hopkinson's law (Baker et al. 1989) which establishes that similar explosive waves are produced at identical scaled distances when two different charges of the same explosive and with the same geometry are detonated in the same atmosphere. Thus, any distance  $R$  from an explosive charge  $W$  can be transformed into a characteristic scaled distance  $Z$ , given by Eq.(1)

$$Z = R/W^{1/3} \quad (1)$$

where  $W$  is the charge mass expressed in kilograms of TNT and  $R$  the distance from the explosive in meters. The corresponding masses for other explosives can be obtained through the concept of TNT equivalence (Formby and Wharton, 1996). The use of  $Z$  allows a compact and efficient representation of blast wave data for a wide range of situations. This law implies that all quantities with dimension of pressure and velocity are unchanged through scaling, i.e. for the same value of  $Z$ .

## 3 NUMERICAL MODEL

### 3.1 Introduction

All the numerical analysis is performed with the hydrocode ANSYS/Autodyn (2009). In order to carry out a comparable analysis, the mass of the explosive is defined by TNT masses. The corresponding masses for other explosives can be obtained through the concept of TNT equivalence.

An Euler Godunov multi material with strength higher order processor (Autodyn 2009) is used to model the problems including the air, the explosive charge and the soil.

### 3.2 Material models

The ideal gas equation of state is used for the air. Lee-Tarver equation of state (Lee and Tarver, 2008) is used to model both the detonation and expansion of TNT in conjunction with “Jones - Wilkins - Lee” (JWL EOS) to model the unreacted explosive.

A shock equation (Autodyn 2005) of state is used for the soil. The initial density is taken as  $\rho = 2.2 \text{ g/cm}^3$  (wet density). The wet density is obtained considering a mean dry density of  $2100 \text{ kg/m}^3$  and a moisture content of 5%.

It has been experimentally proved that for most solids and many liquids there is a linear relationship between the shock velocity  $U$  and the material velocity behind the shock  $u_p$  over a wide range of pressure,

$$U = c_o + su_p \quad (2)$$

Where  $c_o$  is sound speed.

The Mie-Gruneisen form of equation of state based on the shock Hugoniot is used,

$$p = p_h + \Gamma \rho (e - e_h) \quad (3)$$

Where  $e$  is the internal energy,  $\rho$  is the density and  $\Gamma$  is the Gruneisen Gamma, defined as,

$$\Gamma = v \left( \frac{\partial p}{\partial v} \right)_v \quad (4)$$

$p$  is the pressure and  $v$  the specific volume.

It is assumed that  $\Gamma \rho = \Gamma_o \rho_o = \text{constant}$  and

$$p_h = \frac{\rho_o c_o^2 \mu (1 + \mu)}{[1 - (s-1)\mu]^2} \quad (5)$$

$$e_h = \frac{1}{2} \frac{p_h}{\rho_o} \left( \frac{\mu}{1 + \mu} \right) \quad (6)$$

where  $\mu = \frac{\rho}{\rho_o} - 1$

The assumption of constant  $\Gamma \rho$  is probably not valid. Furthermore, the assumption of a linear variation between the shock velocity  $U$  and the particle velocity  $u_p$  does not hold for

too large compression pressure. At high shock strengths some nonlinearity in this relationship is apparent, particularly for non-metallic materials. This non linearity can be covered by a smooth interpolation between two linear relationships or by a quadratic shock velocity (Autodyn 2005).

An elastoplastic strength model based on Drucker Prager criterion and a hydro tensile limit are also used for the soil. The yield stress is a piecewise linear function of pressure. A summary of soil properties used for soil is presented in Table 2.

The accuracy of numerical simulations of craters produced by explosions on the soil surface (Ambrosini and Luccioni, 2006) and underground explosions was proved (Luccioni et al., 2009, Luccioni and Ambrosini, 2008) in recent papers. Although the blast wave generated in soil is strongly dependent on soil model and properties (Luccioni and Ambrosini, 2008), elastic properties, failure limit and yield function of the soil do not significantly affect diameter of the crater obtained (Ambrosini and Luccioni, 2006, Luccioni et al., 2009).

Equation of State: Shock	Strength: Drucker Prager	
Reference density $\rho = 2.2 \text{ g/cm}^3$	Shear Modulus $G = 2.4 \cdot 10^5 \text{ kPa}$	
Gruneisen Gamma $\Gamma = 0.11$	Pressure 1 = $-1.149 \cdot 10^3 \text{ kPa}$	Yield stress 1 = $0 \text{ kPa}$
$c_o = 1.614 \cdot 10^3 \text{ m/s}$	Pressure 2 = $6.88 \cdot 10^3 \text{ kPa}$	Yield stress 2 = $6.2 \cdot 10^3 \text{ kPa}$
$S = 1.5$	Pressure 3 = $1.0 \cdot 10^{10} \text{ kPa}$	Yield stress 3 = $6.2 \cdot 10^3 \text{ kPa}$
	Hydro tensile limit $p_{min} = -100 \text{ kPa}$	

Table 2: Soil properties

### 3.3 Boundary conditions

Flow out of air and TNT en Euler meshes border is allowed to represent unlimited air medium for blast wave propagation problems.

In order to fulfil the radiation condition, a transmitting boundary is defined for soil subgrids external limits. The transmitting boundary condition allows a stress wave to continue “through” the physical boundary of the subgrid without reflection. The transmit boundary is only active for flow out of a grid. Air and TNT flow through grid sides is also allowed over the ground level. The size of the numerical mesh can be reduced using this type of boundary condition. Nevertheless, the boundaries should not be close to the crater because the transmit boundary is only an approximation and some spurious wave reflections could be expected to take place on boundaries.

## 4 BLAST WAVE PROPAGATION

### 4.1 Introduction

The behavior of blast waves in congested urban environments is both difficult to predict and of great importance in assessing explosion effects on buildings and people. Empirical equations are not applicable to this case because they are not able to take into account multiple blast wave reflections on obstacles. Full scale tests of this type of problem are almost prohibitively expensive and require too much time. As a result, this type of problem is often experimentally studied using reduced scale tests.

Alternatively, the problem can be numerically simulated using hydrocodes. It is well known that the accuracy of numerical results is strongly dependent on the mesh size used for the analysis. On the other side, the mesh size is also limited by the dimensions of the model and the computer capacity. One of the major features in the numerical simulation of blast wave propagation in large urban environments is the use of an adequate mesh size.

The validity of blast wave propagation results obtained from small scale test is numerically proved in this section. Moreover, the effect of mesh size when the numerical problem is scaled down is addressed.

#### 4.2 Free field blast wave propagation

When a condensed high explosive is detonated, a blast wave is formed. It is characterized by an abrupt pressure increase at the shock front, followed by a quasi-exponential decay back to ambient pressure and a negative phase in which the pressure is less than ambient pressure. There are many solutions for the wave front parameters produced by spherical explosives from both numerical simulations and experimental measurements (Kinney and Graham, 1985, Smith and Hetherington, 1994). The results are usually presented in graphics, tables or equations based on experimental or numerical results, such as Eq. (7) presented by Kinney and Graham (1985),

$$\frac{p_s}{p_o} = \frac{808[1 + (Z/4.5)^2]}{\sqrt{1 + (Z/0.048)^2} \sqrt{1 + (Z/0.32)^2} \sqrt{1 + (Z/1.35)^2}} \quad (7)$$

where  $t$  is the time,  $p_o$  is the ambient pressure,  $p_s$  is the peak overpressure.

The accuracy of predictions and measurements in the near field is lower than in the far field, probably due to the complexity of blast phenomena (Smith and Hetherington, 1994). This observation is particularly important for large explosions where even large stand off distances give small scaled distances, see Eq (1).

It may be observed that Eq.(7) states that the peak overpressure value is only function of the scaled distance  $Z$ . That is, if the problem is scaled following Table 1, dimensions and distances are reduced by factor  $s$ . As the density is assumed constant, explosive mass will be reduced by a factor  $s^3$  and, thus, the scaled distance remains constant. So the same peak overpressure value is expected to be obtained.

The problem of free air blast wave propagation was numerically solved in two different scales. Assuming scale factor  $s = 5$ , the following cylindrical (height/diameter=1) explosives loads were simulated  $W = 1000\text{kg TNT}$  and  $W^s = W / s^3 = 8\text{kg TNT}$

Due to symmetry conditions free air blast wave propagation was studied with 2D cylindrical models. The analysis of the blast wave propagation was performed in two stages. The first part of the analysis consists of the simulation of the explosion itself from the detonation instant with a very fine mesh. In the second part, the results of the first part are mapped on to a coarser mesh to simulate the propagation of the blast wave generated by the explosion. The model used for the numerical simulation for the second part of the analysis in the case of the full scale problem is presented in Fig.1. Three mesh sizes: a) 50cm, b) 20cm and c) 10cm were used for the full scale problem. For the small scale problem, the model was completely scaled down using scale factor  $s = 5$ . In order to simulate a free field explosion, flow out of air was allowed in all the model borders. Nevertheless, it should be observed that

this boundary condition is a numerical approximation and some spurious reflection on borders usually occurs. To avoid the effect of these reflections on numerical values of pressure or impulse the mesh should be enough large.

Numerical results for the peak overpressure with both scale problems and different mesh sizes are compared with those obtained with empirical equation (7) for different scaled distances from the explosive charge in Fig. 2. The results obtained for both problems corresponding to the same mesh refinement are almost coincident. For high-scaled distances the results obtained with the finest mesh are much closer to empirical ones. As the scaled distance decreases, numerical results depart from empirical ones. Nevertheless, it may be noted that the accuracy of empirical relations in the near field is not guaranteed (Smith and Hetherington, 1994). The difference with empirical values is more marked for coarser meshes that give lower values for the peak overpressure, but results tend to converge as the mesh is refined. The results corresponding to the meshes of 100 and 200 mm are almost coincident. It can be concluded that the mesh of 100 mm gives an accurate solution to the full scale problem (20mm for the small scale problem).

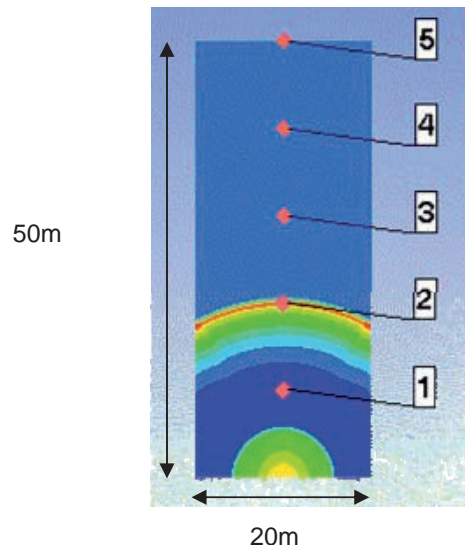


Fig. 1. Numerical model for free air propagation



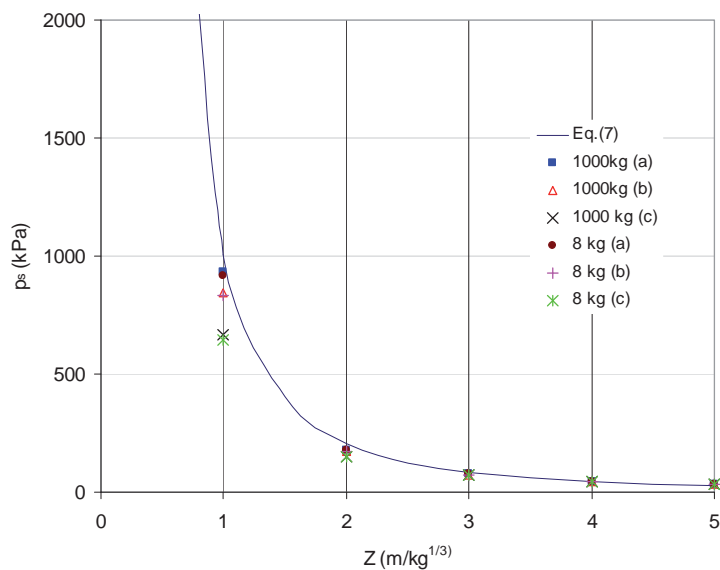


Fig. 2. Peak side-on overpressures as a function of scaled distance.

Fig. 3 shows two pressure–time history curves obtained for point A (see Fig 1), located at 20m from the explosive in the full scale problem (4m in the small scale problem) for the finest mesh. It can be seen that the curves resemble that one previously described. Although both problems give the same overpressure values, time is scaled by a factor  $s$  as was indicated in Table 1. Thus, the arrival time and the duration of the blast wave positive phase are different. As a result, the corresponding impulse values that are obtained integrating the area under the pressure time history are also scaled by a factor  $s$ . For that reason, empirical formulae and tables often give the values of the specific impulse, that is:

$$i_s = I_s / W^{1/3} \tag{8}$$

as a function of  $Z$ . In this case, specific impulse is the same for both problems analyzed. Some little differences can be observed in the blast wave negative phase but they can be attributed to numerical errors.

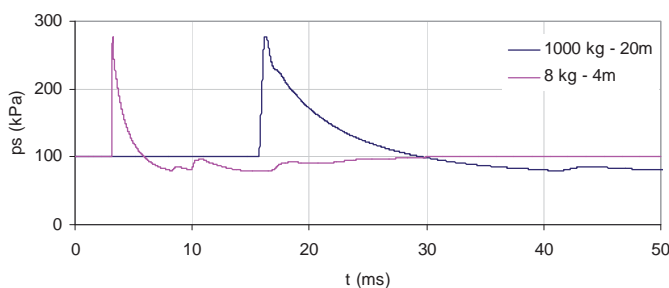


Fig. 3. Pressure–time history.



The comparison of maximum peak overpressures obtained with the finest mesh and experimental results (MacPherson et al., 1999, Smith et al. 2000) is presented in Fig. 4. A good agreement among numerical (finest mesh) and experimental results is observed proving the accuracy of numerical simulation.

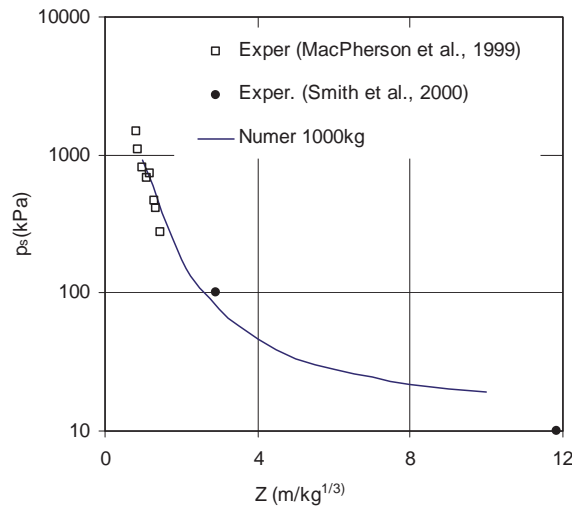


Fig. 4. Comparison of numerical and experimental values of peak side-on overpressures.

### 4.3 Blast wave reflections

When blast waves encounter an infinite large wall on which they impinge at zero angle of incidence, they are normally reflected. All flow behind the wave is stopped and pressures are considerably greater than side-on. The most usual case of loading of large flat surfaces is represented by waves that strike at oblique incidence. For angles of incidence between 0° and 90°, either regular or Mach reflection (Smith and Hetherington, 1994) occurs depending on incident angle and shock strength. The evaluation of reflected pressures resulting from multiple reflections on surfaces with different incidence angles is complex and difficult to perform with empirical equations. In this case, the use of numerical methods is more appropriate. In order to analyze the effect of scaling the problem on reflected pressures and impulses produced by this type of problem, the models presented below is analyzed.

First the effect of blast wave reflections on ground is numerically assessed. The model used for that purpose is represented in Fig 5 for the case of 1000 kg of TNT located at 80cm from the ground. Pressure time histories are registered at the points indicated in Fig. 5, located at 2m from the ground level. Reflection of blast pressure on the ground is considered. The same problem is solved but for the explosive charge of 8 kg of TNT located at 35cm from the ground level and the pressures are registered along the model at a height of 40cm.

Figs 6 and 7 show peak overpressure and specific impulse values as a function of the scaled distance for both scale problems. In case of Fig. 6 the pressure values obtained with TM5 (1986) are also included in the graphic for comparison with numerical results. It can be seen that overpressure values are almost coincident while impulse values are scaled by a factor  $s$ . Nevertheless, if this problem is compared with the problem of free air blast wave propagation it is observed that the small differences obtained between the full scale problem and the small scale problem are greater than in that case and that for long scaled distances the

impulse values are not exactly scaled by  $s$ . These differences can be attributed to reflections on the soil surface.

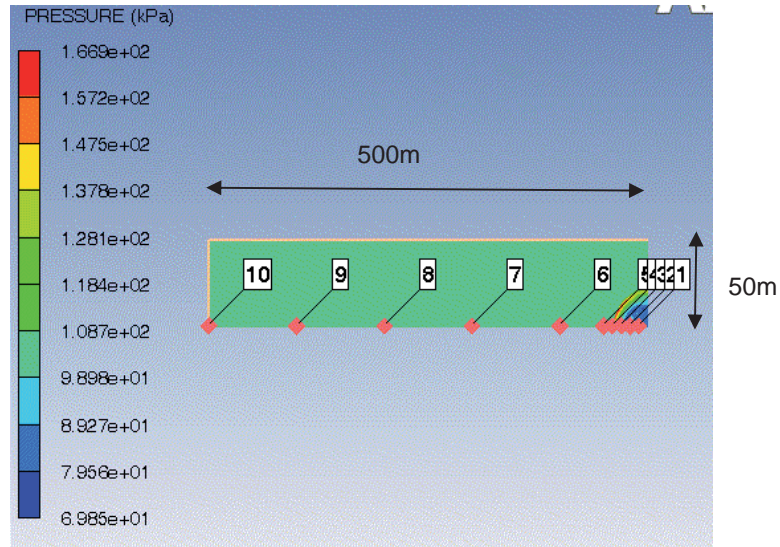


Fig. 5. Model used to simulate blast wave propagation considering ground reflection (full scale problem)

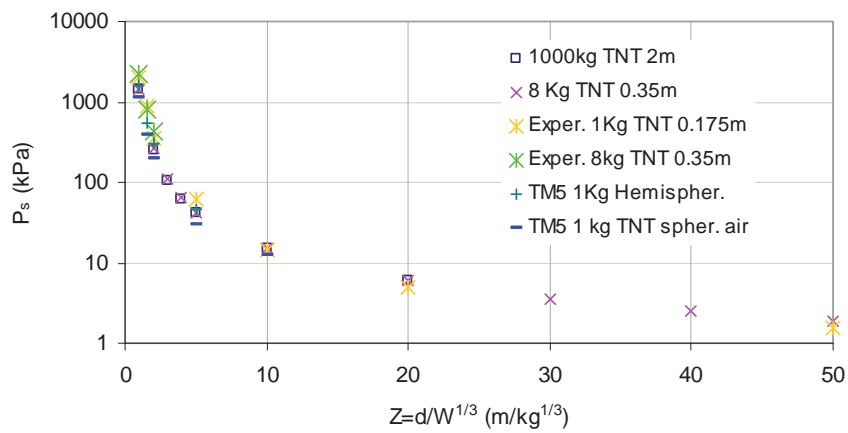


Fig. 6. Peak side-on overpressures as a function of scaled distance.

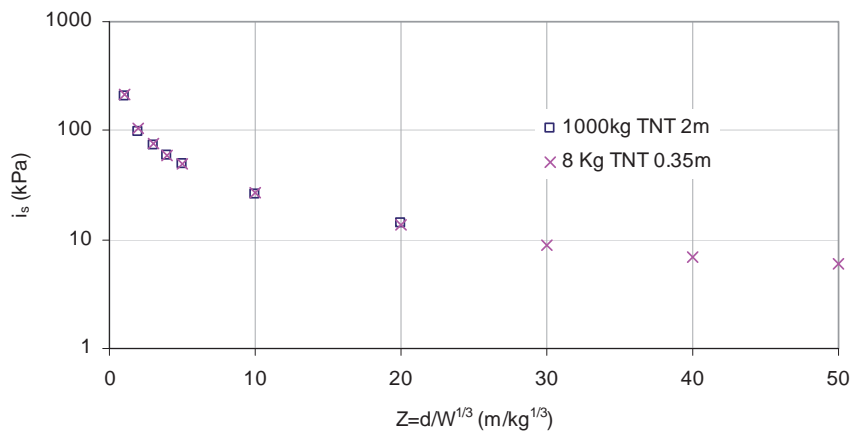


Fig. 7. Peak side-on specific impulse as a function of scaled distance.

The second problem solved is presented in Fig. 8 and corresponds to the blast wave propagation and reflection on a vertical wall. The dimensions in Fig.8 correspond to the full scale problem (1000kg of TNT). For the small scale problem dimensions are scaled down with a factor  $s$ .

Peak reflected overpressure and specific impulse values along a vertical line on the wall (see Fig.8) are presented in Figs 9 and 10 respectively. It can be observed that pressure values are almost coincident except for small differences.

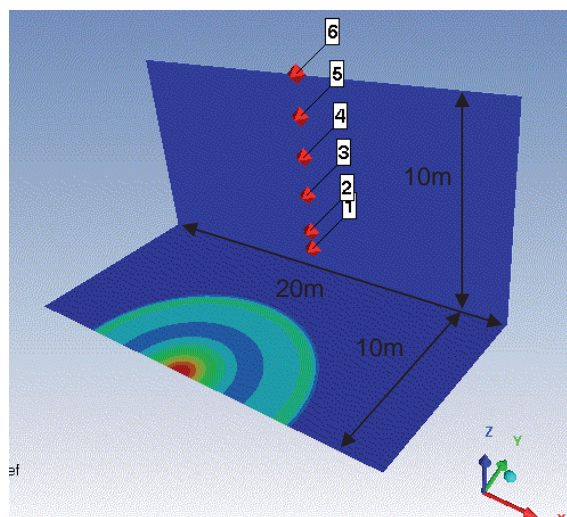


Fig. 8. Model used to simulate blast wave propagation reflection on a vertical wall (full scale problem)

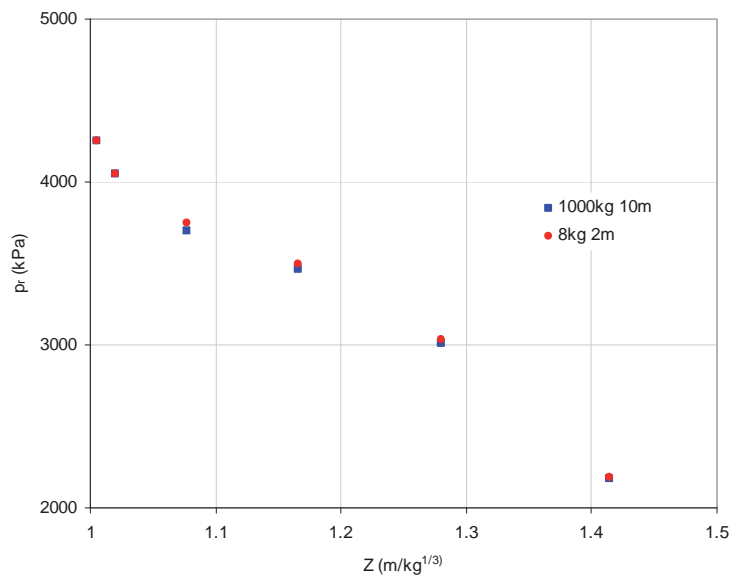


Fig. 9. Peak side-on overpressures as a function of height.

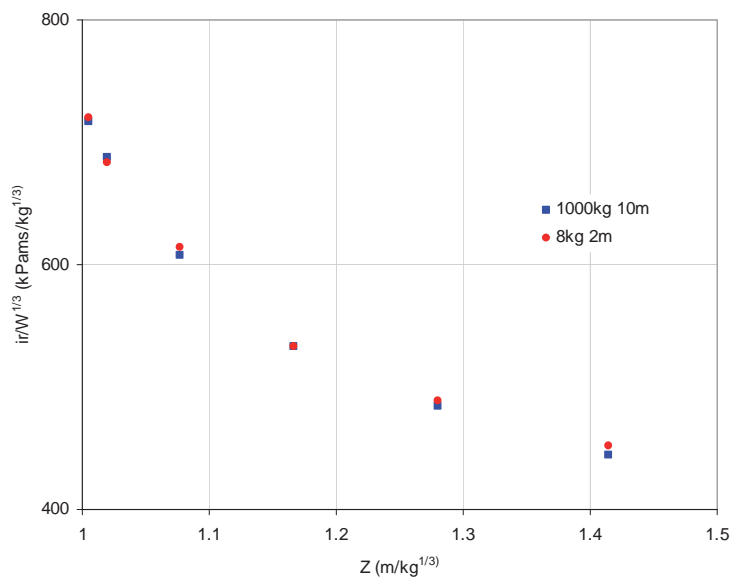


Fig. 10. Peak side-on impulse as a function of height.

All these results confirm the validity of scaling laws presented in section 2 for the explosive range and shape simulated. Nevertheless, previous work (Chung Kim Yuen et al., 2008, Luccioni et al., 2010) show that overpressure values and specific impulse values cannot be represented as a function of the scaled distance  $Z$  defined by Eq.(1) when the explosive load is spread in carpet like form. The use of a modified scale distance defined as :

$$Z' = R/W^{1/4} \quad (9)$$

is suggested. In contrast with the scaled distance defined by Eq.(1), the values of  $Z'$  are not longer preserved when the problem is scaled down using the relationships presented in Table 1.

## 5 CRATER FORMATION

A cavity is always formed when a confined explosion is produced in a mass of soil. If the explosion is close to the surface, a crater is formed, a complex interaction taking place between gravity effects, soil strength and transient load conditions. The most important variables in defining the crater shape and size are the mass  $W$  of the explosive and the depth of the detonation beneath the air/soil interface  $d$ .

The scaling law establishes that any linear dimension  $L$  of the crater can be expressed as a constant multiplied by  $W^\alpha$  divided by the distance of the charge from the ground, where  $W$  represents the equivalent TNT mass of explosive and  $\alpha$  is a coefficient depending on if the gravitational effects can be neglected or not. In the first case the cubic root law is applicable ( $\alpha = 0.33$ ) and in the other cases the functional dependence can be quite complex.

### 5.1 Craters produced by underground explosions

Baker et al. (1991) present a dimensional study to model the crater formation phenomenon in the case of underground explosions. Six parameters are chosen to define the problem: the explosive mass  $W$ , the depth of the explosive charge,  $d$ , the apparent crater diameter  $D$ , the soil density  $\rho$ , and two strength parameters to define the soil properties: one with the dimensions of a stress  $\sigma$ , related to soil strength, and other with the dimensions of a force divided by a cubic length ( $\text{Nm}^{-3}$ )  $K$ , that takes into account gravitational effects.

After a dimensional analysis and many empirical observations, the following functional relation may be obtained (Baker et al., 1991)

$$\frac{D}{d} = f \left( \frac{W^{7/24}}{\sigma^{1/6} K^{1/8} d} \right) \quad (10)$$

The validity of this equation for explosive in the medium to large range has been proved in a previous paper (Luccioni et al., 2009). In order to assess the applicability of this law for the case of extreme explosive loads and small explosive loads a problem consisting of a 1000kg of TNT explosive load located in a manhole at 50cm depth and cover with a flexible asphalt layer was solved. Then the problem was scaled down with  $s=5$  and scaled up with  $s=1/3$  to obtain the cases of 8kg and 27000 kg of TNT respectively.

The model used for 1000 kg and the crater obtained are shown in Figs 11 and 12 respectively.

The results are plotted in Fig. 13 onto the diagram presented in Luccioni et al. (2009) for comparison with other numerical and experimental results. It is observed that the results follow the same tendency described in Luccioni et al. (2009) even if extreme explosive loads are considered.

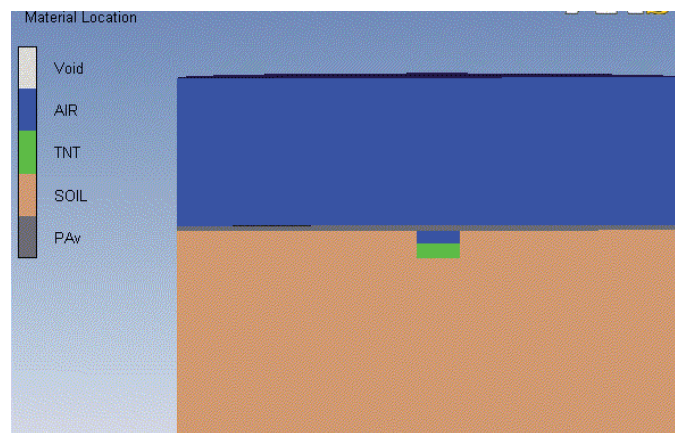


Figure 11. Model used for crater simulation.

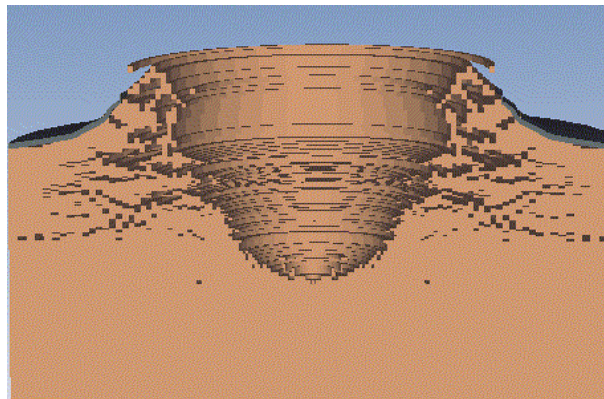


Figure 12. Resulting crater (1000 kg of TNT)



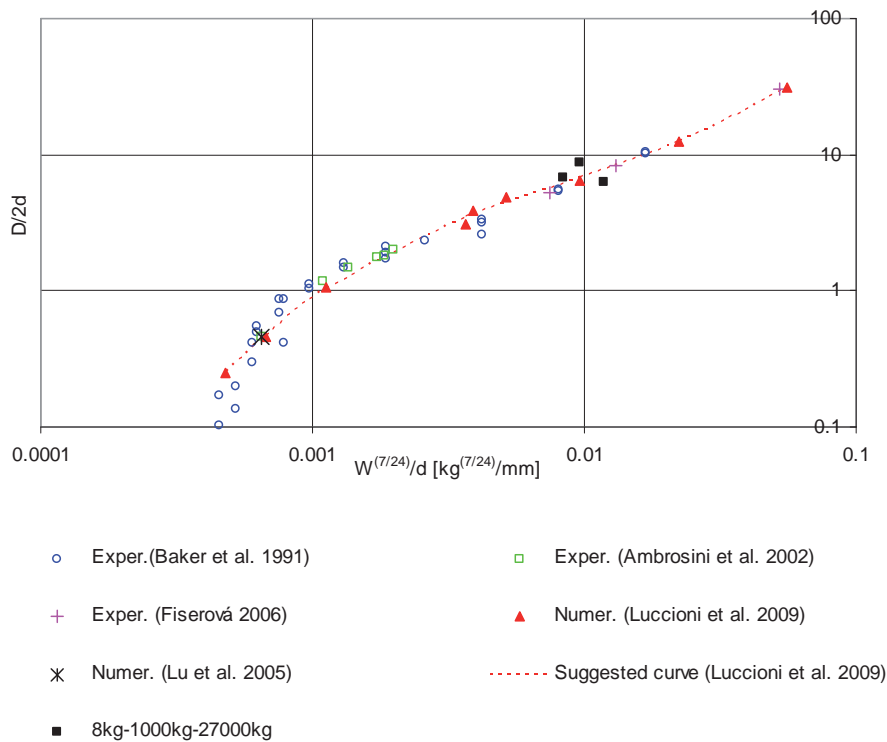


Figure 13. Crater diameter for underground explosions

## 5.2 Craters produced by explosives lying on the ground

Normally, the cubic root scale law has been accepted (Ambrosini and Luccioni, 2006) for craters produced by explosions lying on the soil. In that case, crater diameter is assumed to be proportional to  $W^{1/3}$  and the problem can be directly scaled following Table 1. That is, if the problem is scaled down with a scale ratio  $s$ , the explosive mass will be scaled with  $s^3$ , and  $W^{1/3}$  with  $s$ . According to empirical relationships in Ambrosini and Luccioni (2006), the crater will also be scaled down by a factor  $s$ .

Nevertheless, in a recent paper (Luccioni et al., 2010) the authors have proved that the diameter of craters produced by explosive loads can not longer be assumed to be proportional to  $W^{1/3}$  for the case of explosive loads greater than 1000 kg. Moreover, the relationship between the crater diameter and the mass of explosive strongly depends on the explosive layout.

The crater produced by an explosive load of 1000 kg of TNT lying on the soil is numerically simulated. Two different explosive layouts are considered: a) cylindrical with height / diameter = 1 and b) cylindrical with height / diameter = 0.25.

The problem is scaled down with a factor  $s=5$  (8 kg) and up with a factor  $s=1/3$  ( $W=27000$  kg) and the crater diameter for both explosive layouts is obtained in both cases.

The model used for 1000 kg and the crater obtained are shown in Figs 14 and 15 respectively.

Following the results previously obtained in Luccioni et al. (2010), the crater diameters obtained for all the cases simulated are plotted in Fig.16 as a function of  $W^{1/4}$ . It can be



observed that to cover the complete range of explosive loads simulated the crater diameter can be approximately simulated as a linear function of  $W^{1/4}$  and this function depends on the explosive explosive load shape. Scaling is not longer straightforward in this case. Equations (11) and (12) correspond to two extreme case : carpet like (C) layout and compact (M) (height/diameter=1). The points corresponding to case b) (height/diameter=0.25) fall between the corresponding lines.

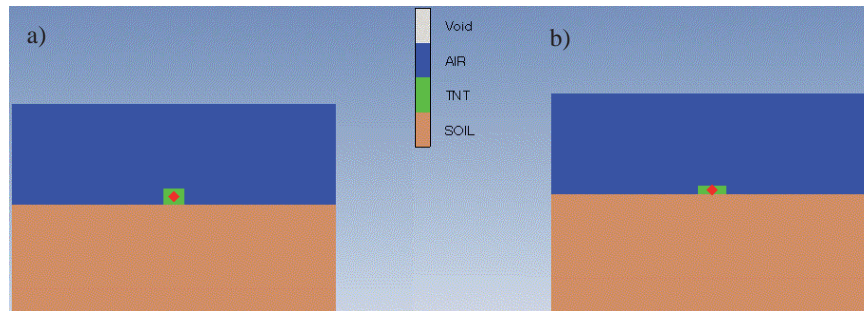


Figure 14. Model used for crater simulation. a) Height/diameter=1; b) Height/diameter=0.25

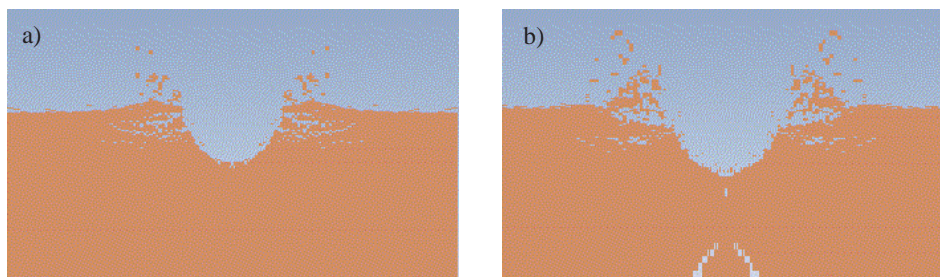


Figure 15. Resulting crater (1000 kg of TNT) . a) Height/diameter=1; b) Height/diameter=0.25

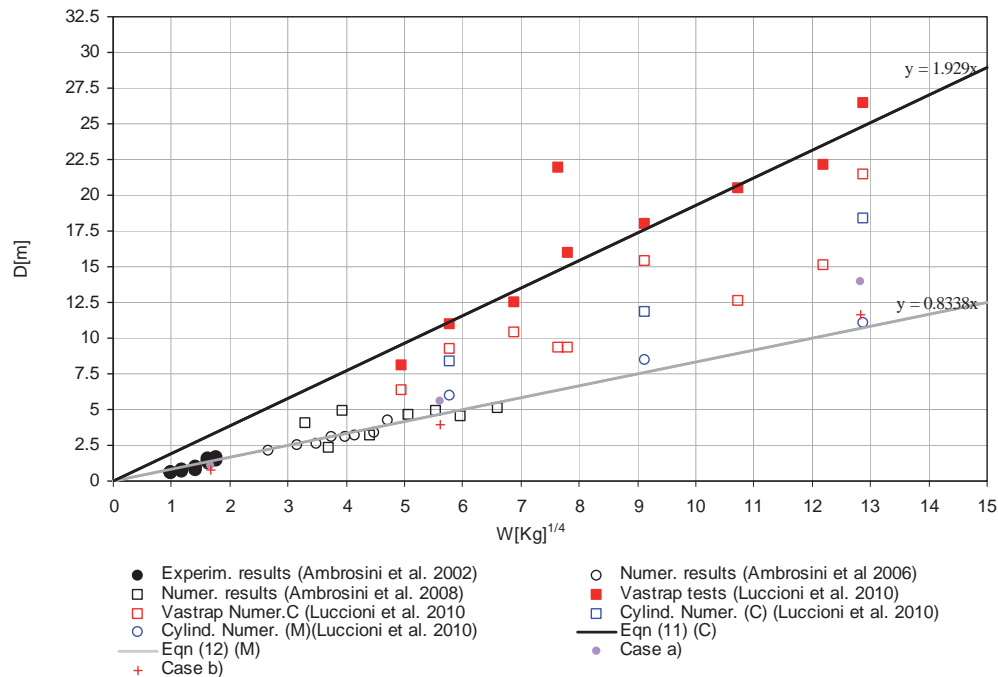


Figure 16. Crater diameter as a function of  $W^{1/4}$

$$(C) D(m) = 1.929W^{1/4} . \tag{11}$$

$$(M) D(m) = 0.834W^{1/4} \tag{12}$$

## 6 CONCLUSIONS

The validity of scaling laws for blast effects was numerically assessed. Two main applications of blast scaling were studied: a) blast wave propagation when some reflections are present and b) crater formation. The accuracy of numerical simulations and numerical results mesh dependence were also analyzed.

The results presented in the paper confirmed that the problem of free air blast wave propagation from a compact shape explosive (spherical or cylindrical with aspect ratio close to unity) can be scaled down using the scaling laws defined in Table 1. Moreover if the numerical problem is scaled, the scaling law should also be applied to the mesh, that is, mesh density should be preserved in order to obtain the same results.

When the problem involves some obstacles that produce blast wave reflections, the obstacles should also be scaled and only very small differences with the full scale problem are expected to be obtained.

In both cases the same overpressure and specific impulse values are obtained. As a consequence, it could be stated that blast load effects can be accurately scaled. Nevertheless this conclusion does not imply that the structure response will be the same. There are many other factors involved in structures response to blast loads that have not be analyzed in this

paper and require further research.

Some limitation of previous conclusions for explosive load with carpet like layout has been shown in the paper. As constant density is assumed, scaling blast effects according to Table 1 implies that the cube root of the mass is scaled with the same factor than linear dimensions and, thus, the same blast effects should be obtained for the same value of  $Z$ . It has been experimentally and numerically proved that this conclusion is not longer valid for explosives spread in a carpet form.

In the case of craters produced by explosive loads the range in which scaling laws described in Table 1 are valid is limited. In this case direct scaling implies that the dimensions of the crater are proportional to the cube root of the explosive mass. It has been proved that this assumption is only valid for the case in which gravitational effects can be neglected, that is up, to 1000 kg of TNT on or above the ground, but can not be extrapolated to extreme explosive loads or underground explosions.

## ACKNOWLEDGEMENTS

The financial support of the CONICET (Argentina) and CIUNT (National University of Tucumán) is gratefully acknowledged.

## REFERENCES

- Ambrosini, R.D., Luccioni, B., Danesi, R., Riera, J. and Rocha, M., Size of Craters Produced by Explosive Charges on or Above the Ground Surface, *Shock Waves*, 12(1), 69-78, 2002.
- Ambrosini, R.D. and Luccioni, B., Craters produced by explosions on the soil surface, *J. Applied Mechanics, ASME*, 73(6), 890-900, 2006.
- Ambrosini, D. and Luccioni, B., Craters produced by large-Scale explosions, *Mecánica Computacional*, XXVI, 1801-1822, 2008.
- ANSYS AUTODYN Version 12.1, User Manual, 2009.
- AUTODYN, Explicit Software for Non-Linear Dynamics, Theory Manual, Revision 4.3, Century Dynamics Inc, 2005.
- Baker, W.E., Cox, P.A., Westine, P.S., Kulesz, J.J. and Strehlow, R.A., *Explosion hazards and evaluation*, Elsevier; 1983.
- Baker, W.E., Westine, P.S. and Dodge, F.T., *Similarity methods in engineering dynamics*. Amsterdam: Elsevier; 1991.
- Chung Kim Yuen, S., Nurick, G.N., Verster, W. Jacob, N., Vara, A.R., Baldena, V.H. , Bwalya, D., Govender, R.A., Pittermann, R.A. Deformation of mild steel plates subjected to large-scale explosions. *International Journal of Impact Engineering*, 35:684–703, 2008.
- Fišerová D, Numerical analyses of buried mine explosions with emphasis on effect of soil properties on loading, Ph.D. Thesis, Defense College of Management And Technology, Cranfield University, 2006.
- Formby, S.A. and Wharton, R.K., Blast characteristics and TNT equivalence values for some commercial explosives detonated at ground level, *Journal of Hazardous Materials*, 50, 183-198, 1996.
- Hargather, M.J. and G.S. Settles, Laboratory-scale techniques for the measurement of a material response to an explosive blast, *International Journal of Impact Engineering* 36: 940–947, 2009.
- Hargather, M.J., Settles, G.S. and Gatto, J.A., Gram-range explosive blast scaling and associated materials response, *Shock Waves*, Part II, 85-90, DOI: 10.1007/978-3-540-

- 85168-4\_12 , 2009.
- Jones, N., *Structural impact*. Cambridge: Cambridge University Press, 489–519, 1989.
- Kinney, G.F. and Graham, K.J., *Explosive shocks in air*, 2nd ed., Springer Verlag, 1985.
- Kleine1, H. and Takayama, K., Laboratory-scale blast wave phenomena, *Symposium on Interdisciplinary Shock Wave Research Sendai*, Japan, 2004.
- Lee, E.L. and Tarver, C.M. Phenomenological model of shock initiation in heterogeneous explosives. *Physics of Fluids*, 23(12),2362-2372, 2008.
- Luccioni, B., Ambrosini D., Nurick G.N. and Snyman I. Craters produced by underground explosions, *Computers & Structures*, 87,1366-1373, 2009.
- Luccioni, B.M. and Ambrosini D. Evaluating the effect of underground explosions on structures. *Mecánica Computacional*, 27, 1999-2019, 2008.
- Lu Y, Wang Z and Chong K. A comparative study of buried structure in soil subjected to blast load using 2D and 3D numerical simulations. *Soil Dynamics and Earthquake Engineering*, 25:275–288, 2005.
- MacPherson, W.N., Gander, M.J., Barton, J.S., Jones, J.D.C., Owen, C.L., Watson, A.J. et al. Blast-pressure measurement with a high-bandwidth fibre optic pressure sensor. *Measurement Science and Technology*;11: 95–102, 2000.
- Neuberger, Pelesc, S., Rittel, D., Scaling the response of circular plates subjected to large and close-range spherical explosions. Part I: Air-blast loading, *International Journal of Impact Engineering* 34:859–873, 2007a.
- Neuberger, Pelesc, S., Rittel, D., Scaling the response of circular plates subjected to large and close-range spherical explosions. Part II: Buried charges, *International Journal of Impact Engineering* 34:859–873, 2007b.
- Nurick, G.N., Martin , J.B, Deformation of thin plates subjected to impulsive loading – A review .2. Experimental studies. *Int J Impact Eng*;8:171–86, 1989.
- Nurick, G.N., Gelman, M. E., Marshall, N.S., Tearing of blast loaded plates with clamped boundary conditions. *Int J Impact Eng.*;18:803–27, 1996.
- Nurick, G.N., Chung Kim Yuen, S., Jacob, N., Verster, W., Bwalya, D. and Vara, A.R., Response of quadrangular mild-steel plates to large explosive load. *Second international conference on design analysis of protective structures (DAPS)*. Nanyang Technological University, 30–44, 2006.
- Ripley, R.C., von Rosen, B. , Ritzel, D. V. and Whitehouse, D. R., Small-scale modeling of explosive blasts in urban scenarios”, ISB 2004, *21st International Symposium on Ballistics*, Adelaide, Australia, 2004.
- Smith, P.D. and Hetherington, J.G., *Blast and ballistic loading of structures*, Butterworth-Heinemann Ltd; 1994.
- Smith, P.D., Rose, T.A. and Saotonglang, E., Clearing of blast waves from building facades. *Proceedings of Institution of Civil Engineers: Structures & Buildings*;134:193–9, 1999.
- US Army (1986). TM 5-855-1 Fundamentals of Protective Design for Conventional Weapons, US Army Waterways Experimental Station.